

ANALYSIS OF SURFACE RUPTURE PATTERNS AND FAULT OFFSET VARIABILITY ASSOCIATED WITH THE 06 FEBRUARY 2023 PAZARCIK (KAHRAMANMARAS) EARTHQUAKE (MW 7.7) IN ISLAHIYE AREA, TURKIYE

A. Caglayan^{1*}, V. Isik², R. Saber³, H. Unal⁴, F. Chitea^{5,6}

¹*Dr., Department of Geological Survey, Ministry of Environment, Urbanisation and Climate Change, General Directorate of Spatial Planning, Ankara, Turkiye*

²*Prof. Dr., Department of Geological Engineering, Ankara University, Ankara, Turkiye*

³*Dr., Department of Geological Engineering, Ankara University, Ankara, Turkiye*

⁴*Mr., Geomek Mühendislik, Geoteknik, Proje, Ankara, Turkiye*

⁵*Lect. Dr., Department of Engineering Geology and Geophysics, Bucharest University, Bucharest, Romania*

⁶*Lect. Dr., Institute of Geodynamics of the Romanian Academy, Bucharest, Romania*

Email: ayse.caglayan@csb.gov.tr

ABSTRACT

Numerous destructive earthquakes have occurred in Turkiye, part of the Alpine-Himalayan Orogenic Belt, both in historical and instrumental periods, resulting in many appalling causalities. Pazarcık earthquake (Mw 7.7), the first major earthquake of the 06 February 2023 Kahramanmaraş earthquake sequences, occurred along the so-called East Anatolian Fault Zone. A total surface rupture was approximately 250 km long from Golbası to Antakya. A maximum left-lateral offset of 4-4.5 m has been documented, with various dip-slip displacements from tens of cm to a few meters. The overall direction of surface rupture changes noticeably from NE to SE, forming NW-facing arc-shaped geometry. The evidence of surface faulting is traceable along hillslopes, valleys and plain terrain, as well as on modern manufactured structures such as roads, garden walls, houses and barns.

Various well-developed surface faulting geometries were observed in field studies, high-resolution satellite images, and UAV-based aerial photos. Different morphological features, including simple and complex fault traces, pop-up structures, sag ponds, fault splays and lateral spreading related to surface deformation, were observed in the Islahiye area. The lateral width of the surface ruptures varies from a few to a hundred meters. Formation of typical Riedel fractures is evident in the entire study area, indicating development stages of surface faulting. Left lateral fault offsets were measured, ranging from tens of cm to approximately 3 m, while the vertical displacement was documented to be confined to about 50 cm. Our geological and geomorphological field observations along the active main fault surface indicate that there have been numerous fault activities causing historical and/or prehistorical earthquakes. So far, The results emphasize the importance of adopting risk-based approaches in establishing settlement areas around active fault zones.

KEYWORDS: Twin earthquakes, Surface rupture, Active tectonics, East Anatolian Fault Zone, Southeastern Türkiye

1-INTRODUCTION

The Anatolian Plate, a western domain of the so-called Turkish-Iranian Plateau, includes significant intra-plate deformation zones formed due to the collision of the Arabian and Eurasian Plates (e.g., Şengör and Kidd 1979) (Figure 1). In the literature, different times have been suggested by researchers for the initiation of the collision between the Arabian and Eurasian Plates, such as Late Cretaceous (e.g., Berberian and King 1981), late Eocene to middle Miocene (e.g., Dewey et al. 1986), early Oligocene (e.g., McQuarrie and van Hinsbergen 2013), late Oligocene to late Miocene (e.g., Fakhari et al. 2008) and Pliocene (e.g., Falcon 1974). The most preferred initiation time of the collision is 36–20 Ma (e.g., Zhang et al. 2016), where most of the tectonic responses to the collision occurred after 20 Ma (Su and Zhou 2020). The collision has resulted in the formation of different deformation zones within Anatolia, including the East Anatolian Fault Zone (Arpat and Şaroğlu 1972), North Anatolian Fault Zone (Caglayan et al. 2019), Central Anatolia Deformation Zones (Isik et al. 2014), Western Anatolia Extensional Zones (Isik et al. 2003).

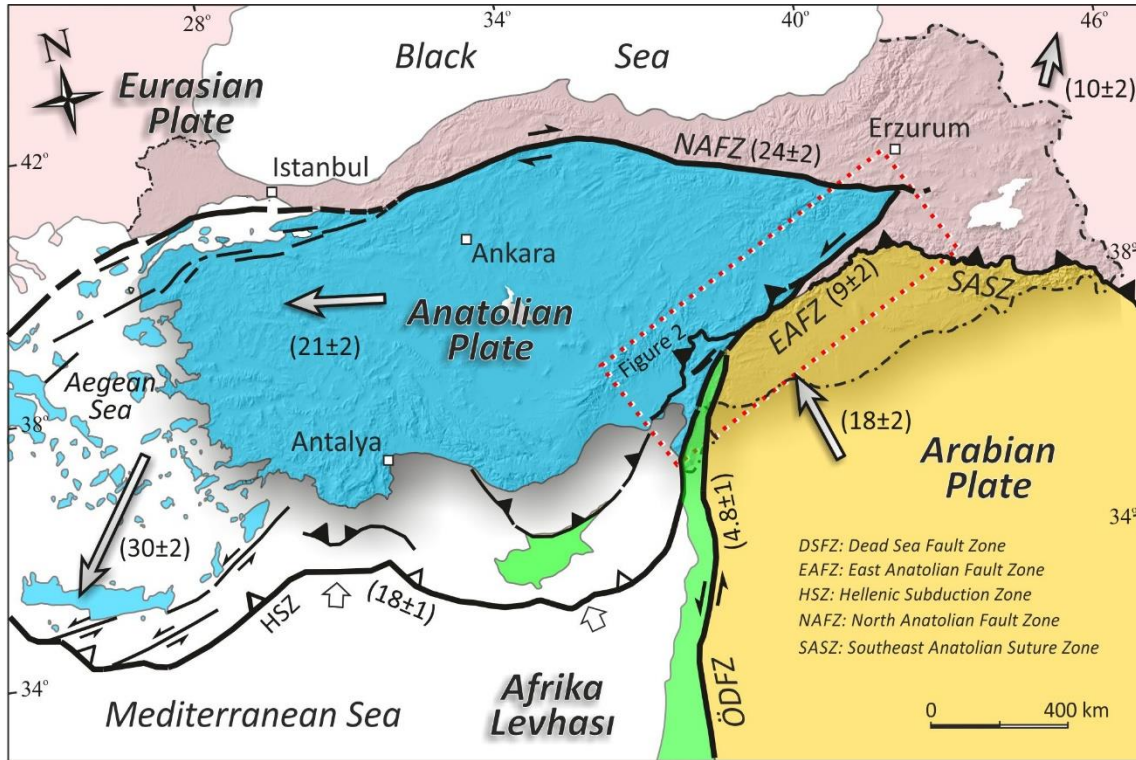


Figure 1. A map showing the interaction between different tectonic plates in Türkiye and the surrounding area.

The East Anatolian Fault Zone (EAFZ) is a major active fault zone in Türkiye that extends for more than 600 kilometers from the Karlıova (Bingöl) to the Mediterranean Sea (e.g. Arpat and Şaroğlu 1972) (Figure 2). The EAFZ is a complex system of faults that includes multiple branches or segments with localized pull-apart basins and push-up zones, with controversial age estimations, likely between Late Miocene-Early Pliocene (e.g., Şengör et al. 1985) or Late Pliocene (e.g., Emre and Duman, 2007) and slip rate of 6 mm/yr to 10 mm/yr. (Taymaz et al. 1991). Historical and instrumental records reveal significant seismic activity along the EAFZ. The largest known historical earthquakes along the EAFZ occurred on November 29, 1114 (M

> 7.8), March 28, 1513 ($M > 7.4$) and March 2, 1893 ($M > 7.1$) (Ambraseys and Jackson 1998). In contrast, these large devastating historical earthquakes contrast with few significant earthquakes during the last century on December 4, 1905 Mw 6.8 earthquake (Nalbant et al., 2002), January 24, 2020 Mw 6.8 earthquake (Pousse-Beltran et al. 2020), and lately destructive February 06, 2023 Mw: 7.8 Earthquake. The latter earthquake has produced a surface rupture of more than 300 km in length from north of Gölbaşı (Adıyaman) to the Antakya (Hatay) in the SW. The remote sensing observations revealed the curved shape and complex nature of the surface rupture.

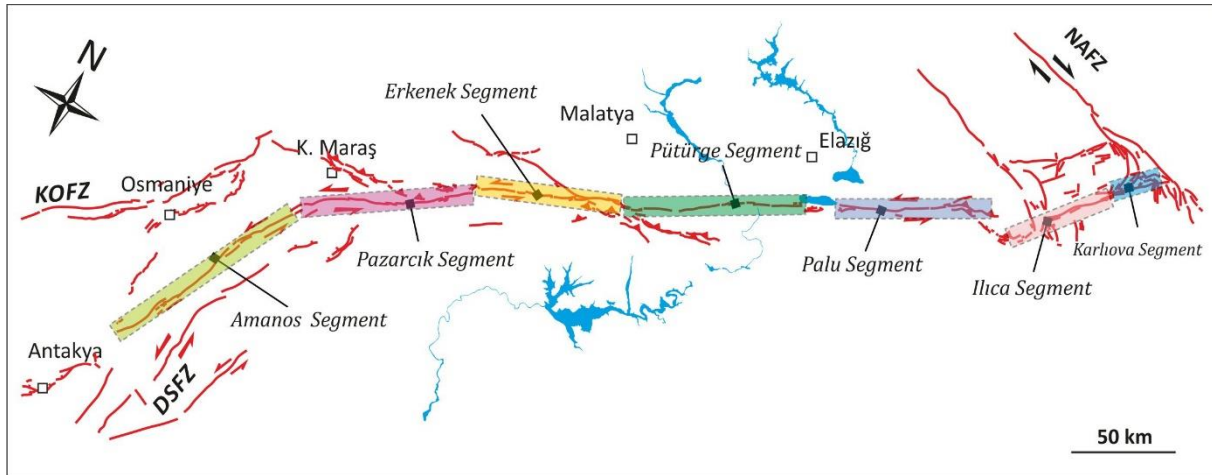


Figure 2. A map showing different fault segments of the East Anatolian Fault Zone.

In this study, an optical post-event satellite image investigation was conducted to obtain the whole distribution of co-seismic surface rupture by using high-resolution Maxar images. After determining the location of possible ruptures derived from satellite images, the field survey was carried out with a high-precision mapping drone, and the surface rupture data were gathered. Subsequently, all collected data were processed to measure fracture patterns and fault offset amounts.

2-METHOD and APPLICATION

The study included two stages: office-based remote sensing studies and field surveys. Firstly, resolution precious Maxar optical images were acquired on February 08, 2023 and are available online for research purposes. Using Maxar images, the surface ruptures were generally mapped, and the potential locations for field observation, drone flight areas and detailed mapping were selected. A DJI Phantom 4 RTK (real-time kinematic) drone with vertical positioning accuracy of 1.5 cm + 1 ppm and a ground resolution of 2.74 cm at a 100 m flight altitude was used for photogrammetry studies. All captured digital images were imported into Agisoft Metashape 1.8.5 software. The software automatically recognizes the relative position and direction of each photo, calculates the aerial triangulation and performs 2D and 3D reconstructions using the generated point cloud data. As a result, DEMs, DSMs, orthophotos, and 3D models could be extracted from processed data. Finally, detailed surface rupture maps along the study area were generated.

3-RESULTS

The surface deformation map shows that the main area impacted by the Pazarcık earthquake in the Islahiye area is approximately 6×12 km. The rupture zone presents two main fault branches propagating in the SW direction (Figure 3). This is consistent with the preexisting tectonic landforms, morphological features and outcrop evidence of fresh and relatively older fault

slickensides, suggesting the repetition of several destructive historical earthquakes in the study area. Left lateral fault offsets were measured, ranging from tens of cm to approximately 3 m. while the vertical displacement was documented to be confined to about 50 cm. (Figure 3). Continuous rupture traces with lengths ranging from several meters to tens of meters were observed in the field investigations. Based on the branching of the fault strike, the surface rupture of the earthquake in this area can be roughly divided into two sections. The western section, which has a strike of N30°E to N70°E, consists of intermittent fractures with different lengths. The eastern fault branch strikes N25°-30°E and has a length of ~10 km with highly discontinuous and intermittent geometry (Figure 3)

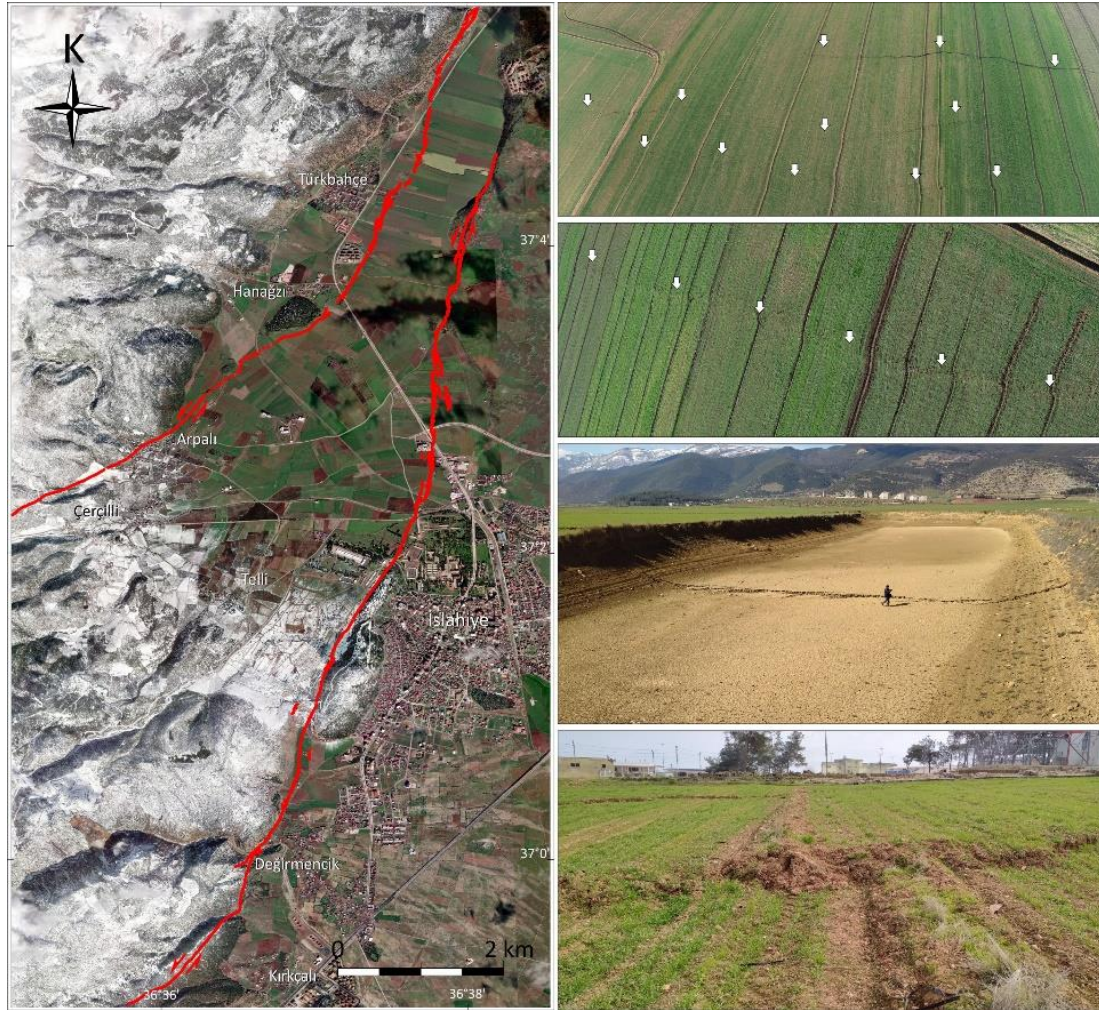


Figure 3. Maxar satellite image (left), and field and drone images (right) of surface faulting along the Islahiye area.

In the Islahiye area, surface faulting is mainly characterized by simple shear on the surface, representing various Riedel fractures arranged in en-echelon geometries (Figures 4 and 5). Various types of Riedel fractures and morphological features, such as push-up and small-scale pull-apart structures, were found in field observations and laboratory studies. On the obtained orthophotos, all the fracture strikes were measured and projected onto the rose diagram (Figures 4 and 5). Comparison of The results indicate two main distribution types of rupture patterns. The first type is R, P and T, with a minority of R' Riedel fractures. The angular difference between main populations of fractures with principal displacement zone does not exceed 15°-20°, demonstrating nearly linear propagation of surface faulting.

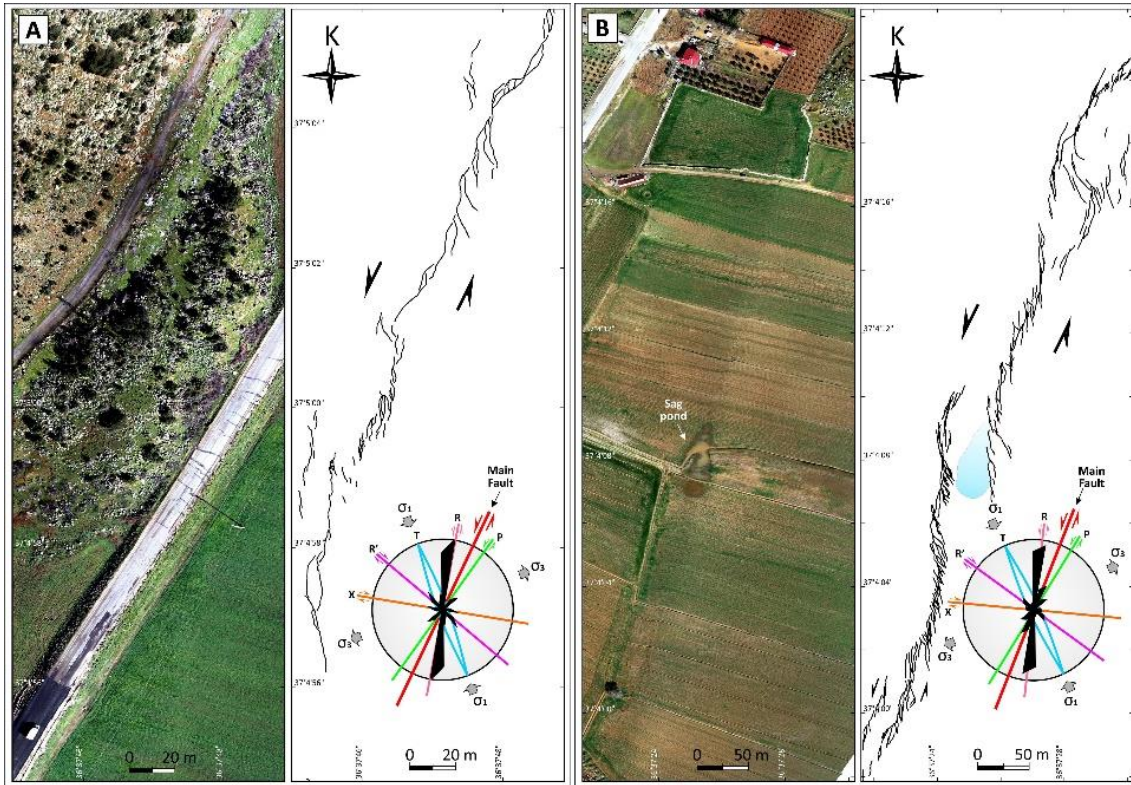


Figure 4. Orthophotos and sketch drawings of surface ruptures on the western fault branch during the Pazarcık earthquake.

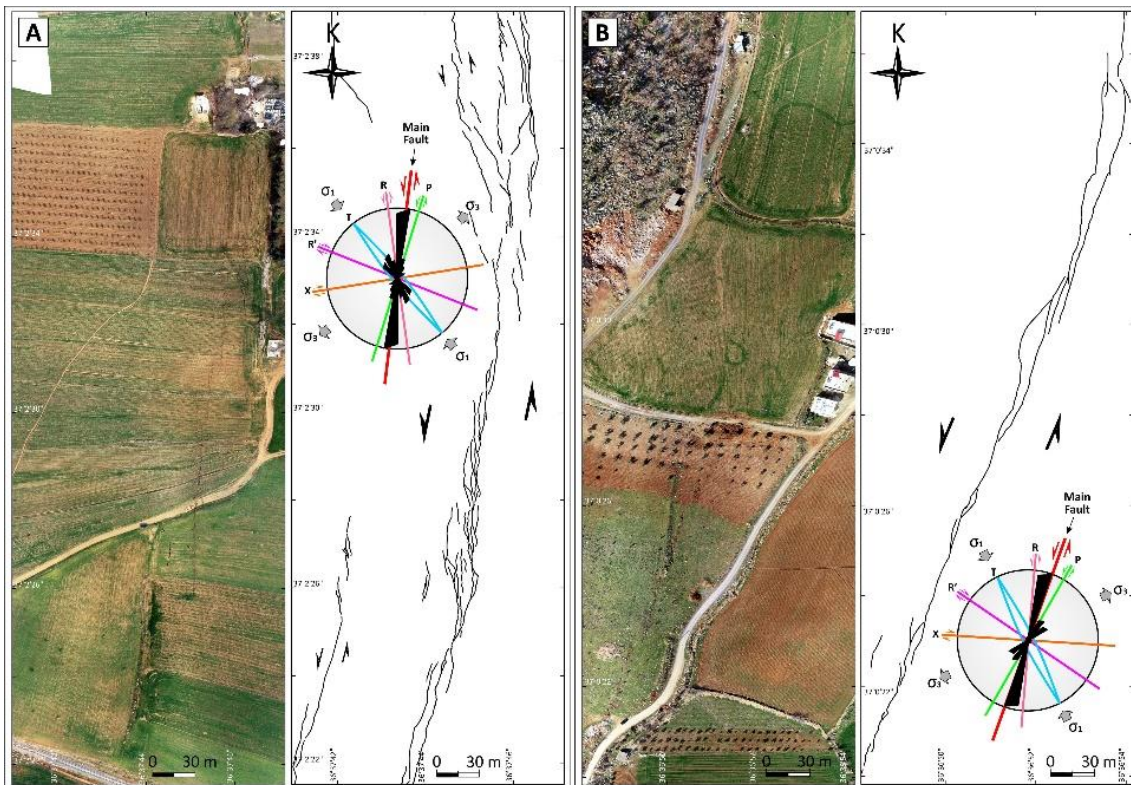


Figure 5. Orthophotos and sketch drawings of surface ruptures on the eastern fault branch during the Pazarcık earthquake.

The second type indicates that the several meters to several tens of meters long en-echelon shears represent major structures along the study area (Figures 4 and 5). The angular difference between the orientations of the en-echelon shears and the principal displacement zone is 20°–30°. The fault stepping along the surface ruptures have formed several typical push-up and sag pond structures (Figures 4 and 5). Finally, drone observations reveal that geomorphological features such as ruts, gullies, and streams and modern structures such as roads, walls, and buildings were displaced horizontally and vertically by a fault along the rupture zone (Figures 4 and 5). These indicate that the Pazarcık earthquake resulted in a primarily left-lateral strike-slip motion.

4-CONCLUSIONS

The main conclusions reached in this study are:

1. Different morphological features, including simple and complex fault traces, pop-up structures, sag ponds, fault splays and lateral spreading related to surface deformation, were observed in the Islahiye area. The lateral width of the surface ruptures varies from a few to a hundred meters. The lateral width of the surface ruptures varies from a few to a hundred meters.
2. Formation of typical Riedel fractures is evident in the entire study area, indicating development stages of surface faulting. The R, P and T, with a minority of R' Riedel fractures, are dominant fractures along the study area. The several meters to several tens of meters long en-echelon shears represent major structures also.
3. Left lateral fault offsets were measured, ranging from tens of cm to approximately 3 m, while the vertical displacement was documented to be confined to about 50 cm.
4. The consistency between surface faulting with the preexisting tectonic landforms, morphological features and outcrop evidence of fresh and relatively older fault slickensides, suggesting the repetition of several destructive historical earthquakes in the study area.

5-REFERENCES

- Ambraseys, N.N., Jackson, J. A. 1998. Faulting is associated with historical and recent earthquakes in the Eastern Mediterranean region. *Geophys. J. Int.*, 133, pp. 390–406.
- Arpat, A. E., Şaroğlu, F. 1972. Doğu Anadolu Fayı ile ilgili bazı gözlem ve düşünceler. *Bulletin of the Mineral Research and Exploration*, 73, 1–9.
- Berberian, M., King, G. 1981. Toward a paleogeography and tectonic evolution of Iran. *Canadian Journal of Earth Science* 18, 502–557.
- Caglayan, A., Isik, V., Saber, R. 2019. Paleoseismologic evidence for Holocene activity on 1944 earthquake segment, north Anatolian fault zone. *Geoscience Journal*, 23, 805–22. <https://doi.org/10.1007/s12303-018-0075-3>.
- Dewey, J.F., Hempton, M.R., Kidd, W.S.F., Şaroğlu, F., Şengör, A.M.C. 1986. Shortening of continental lithosphere: the neotectonics of Eastern Anatolia a young collision zone. In "Collision tectonics" eds. M. P. Coward and A. C. Ries, *Geol. Soc. Spec. Publ.*, 19, pp. 3-36.
- Emre, O., Duman, T.Y., 2007. The East Anatolian Fault: Structural Pattern and Relationship with the Dead Sea Transform. *American Geophysical Union, Fall Meeting 2007, Abstract #T42B-01*.

- Fakhari, M., Axen, G., Horton, B., Hassanzadeh, J., Amini, A. 2008. Revised age of proximal deposits in the Zagros foreland basin and implications for Cenozoic evolution of the high Zagros. *Tectonophysics* 451, 170–85.
- Isik, V., Seyitoglu, G., Cemen, I., 2003. Ductile–brittle transition along the Alas, chir detachment fault and its structural relationship with the Simav detachment fault, Menderes Massif, western Turkey. *Tectonophysics* 374, 1–18.
- Isik, V., Uysal, I. T., Caglayan, A., Seyitoglu, G. 2014. The evolution of intraplate fault systems in central Turkey: structural evidence and Ar–Ar and Rb–Sr age constraints for the Savcili Fault Zone. *Tectonics* 33, 1875–99. <https://doi.org/10.1002/2014TC003565>.
- McQuarrie, N., van Hinsbergen, D. 2013. Retrodeforming the Arabia–Eurasia collision zone: age of collision versus magnitude of continental subduction. *Geology* 41, 315–8.
- Nalbant, S., McCloskey, J., Steacy, S., Barka, A. 2002. Stress accumulation and increased seismic risk in eastern Turkey. *Earth Planetary Science Letters* 195, 291–298.
- Pousse-Beltran, L., Nissen, E., Bergman, E. A., Cambaz, M. D., Gaudreau, E., Karasözen, E., Tan, F. (2020). The 2020 Mw 6.8 Elazığ (Turkey) Earthquake Reveals Rupture Behavior of the East Anatolian Fault. *Geophysical Research Letters*, 47 (13), e2020GL088136. doi: 10.1029/2020GL088136.
- Su, H., Zhou, J. 2020. Timing of Arabia–Eurasia collision: constraints from restoration of crustal-scale cross-sections. *Journal of Structural Geology* 135, 104041.
- Şengör, A. M. C. & Kidd, W. S. F. 1979. Post-collisional tectonics of the Turkish–Iranian Plateau and a comparison with Tibet. *Tectonophysics* 55, 361–76.
- Şengör, A. M. C., Görür, N., Şaroğlu, F. 1985. Strike-slip faulting and related basin formation in zones of tectonic escape: Turkey as a case study, *Strike-Slip Deformation, Basin Formation and Sedimentation*. Biddle, K.T., Christie Blick, N. (Eds.), Soc. Eco., Palaeo. Mineral. Spec. Publ., 37, pp. 227–264.
- Taymaz, T., Jackson, J., McKenzie, D. P. 1991. Active tectonics of the north and central Aegean Sea. *Geophysical Journal International*, 106, 433–490.
- Zhang, Z., Xiao, W., Majidifard, M., Zhu, R., Wan, B., Ao, S., Chen, L., Rezaeian, M., Esmaili, R. 2016. Detrital zircon provenance analysis in the Zagros Orogen, SW Iran: implications for the amalgamation history of the Neo-Tethys. *International Journal of Earth Sciences* 106, 1223–38.